

Young black hole and neutron star systems in the nearby star-forming galaxy M33: the NuSTAR view

Jun Yang,^{1,2} Daniel R. Wik,² Ann Hornschemeier,³ Bret Lehmer,⁴ Paul Plucinsky,⁵
Lacey West,⁴ Thomas Maccarone,⁶ Benjamin Williams,⁷ Frank Haberl,⁸ Andrew Ptak,^{3,9} Mihoko Yukita,^{3,9}
Andreas Zezas,^{5,10} Neven Vucic,^{3,11} Vallia Antoniou,⁵ Dominic Walton,¹² and Kristen Garofali⁴

¹Massachusetts Institute of Technology Kavli Institute for Astrophysics and Space Research, Cambridge, MA, United States.

²Department of Physics and Astronomy, the University of Utah, Salt Lake City, Utah, United States. ³ NASA Goddard Space Flight Center, Greenbelt, MD, United States. ⁴ University of Arkansas, Fayetteville, AR, United States. ⁵ Harvard-Smithsonian Center for Astrophysics, Cambridge, MA, United States. ⁶ Texas Tech University, Lubbock, TX, United States. ⁷ University of Washington, Seattle, WA, United States. ⁸ Max-Planck-Institut für extraterrestrische Physik, Garching, Germany. ⁹ The Johns Hopkins University, Baltimore, MD, United States. ¹⁰ University of Crete, Heraklion, Crete, Greece. ¹¹ University of Maryland, College Park, MD, United States. ¹² University of Cambridge, Cambridge, United Kingdom.

Abstract

We can learn a lot about the **formation of compact objects**, such as neutron stars and black holes, by studying the X-ray emission from accreting systems in nearby star-forming galaxies. The harder ($E > 10$ keV) X-ray emission in particular allows strong discrimination among the **accretion states** and **compact object types**. A NuSTAR survey of M33 was conducted to study the distribution of X-ray binary (XRB) accretion states in an actively star-forming environment. The 6 NuSTAR observations of M33 allow us to construct diagnostic diagrams, which is used to infer XRB accretion states. We have characterized XRB accretion states for ~ 28 sources. The XRBs are classified by their compact object types using **NuSTAR color-intensity and color-color diagrams**. We further characterize the **black holes** by their accretion states (soft, intermediate, and hard) and the **neutron stars** by their weak or strong (accreting pulsar) magnetic field.

M33

In the NuSTAR archive, 6 observations are public in the direction of the galaxy M33. There are three fields (each with two separate epochs): Field 1: Observation ID 50310001002 and 50310001004; Field 2: 50310002001 and 50310002003; and, Field 3: 50310003001 and 50310003003.

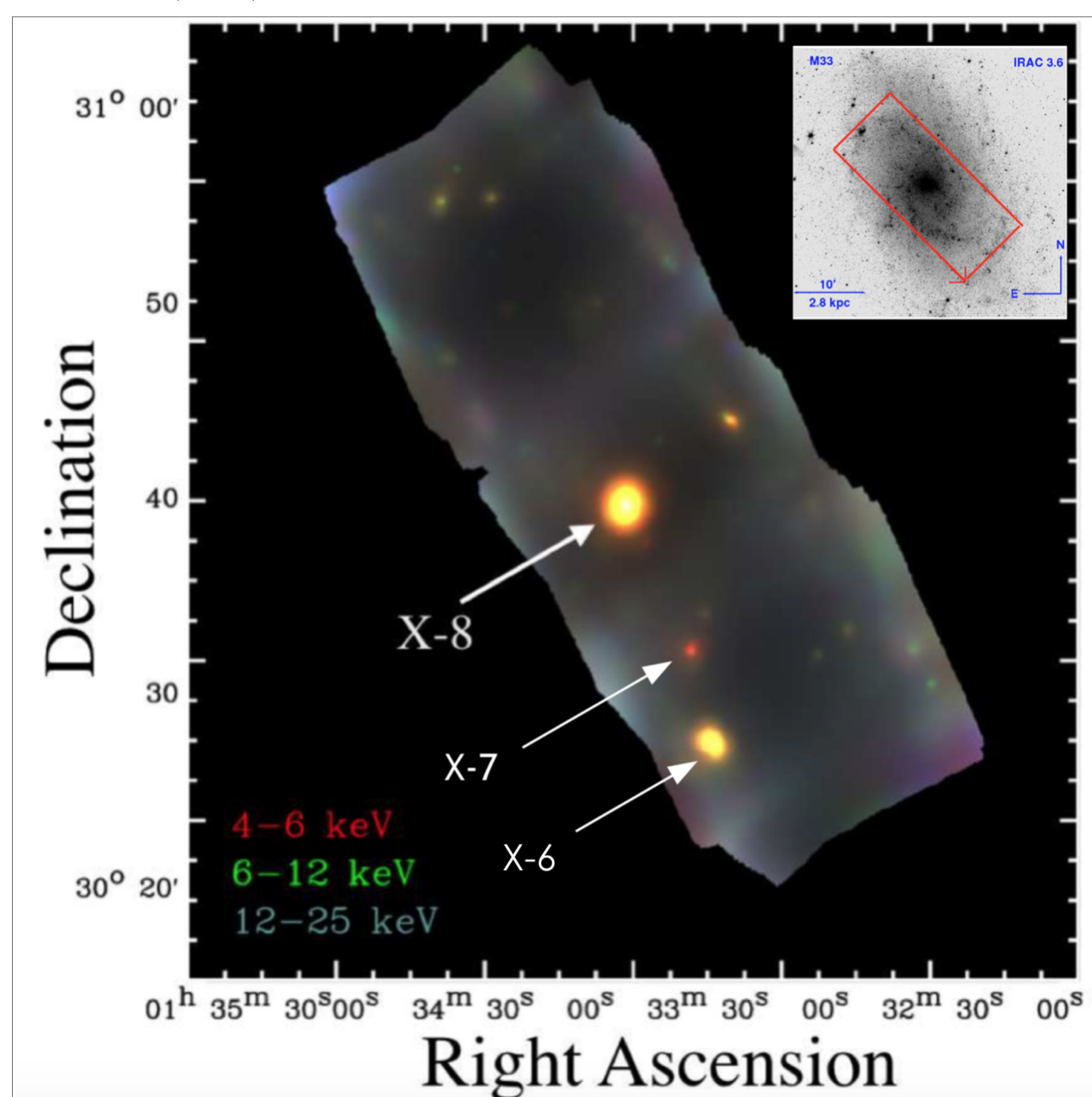


Figure 1: Three-color NuSTAR image mosaic of the M33 legacy fields. The image was constructed from 4–6 keV (red), 6–12 keV (green), and 12–25 keV (blue) exposure-corrected adaptively smoothed images. In the right corner is the Spitzer Infrared Array Camera 3.6 μ m image of M33.

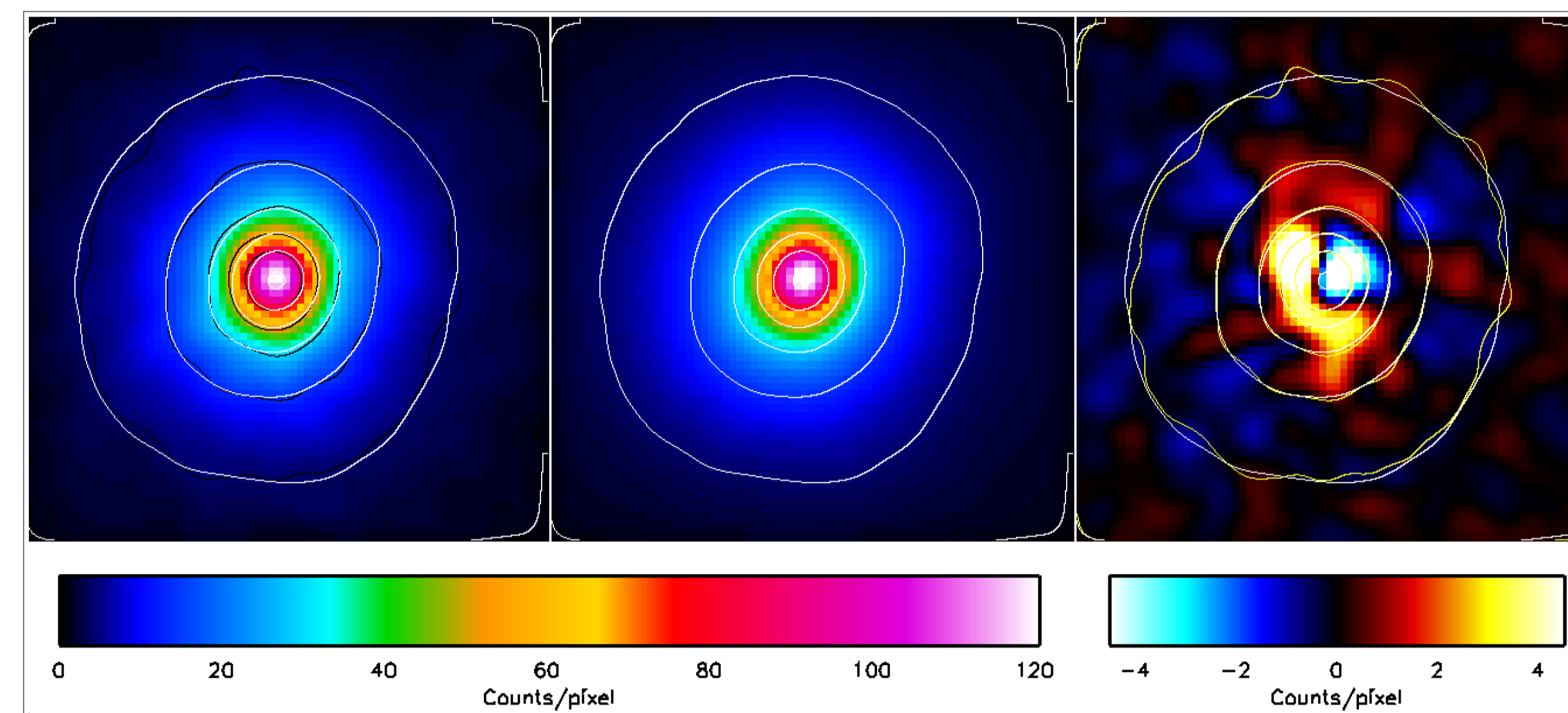


Figure 2: Point spread function calibrated point source image fits for M33 X-8: **left** panel displays smoothed, **background-subtracted** count data from both epochs. **Middle** panel is the best-fit **model**, and the white contours in all the three panels outlines the smoothed model image. The **right** panel shows the **residual** between data and model with a smaller color scale color bar. The yellow contours presents the data. Both the yellow and white contours present identical intensities.

NuSTAR diagnostic diagram

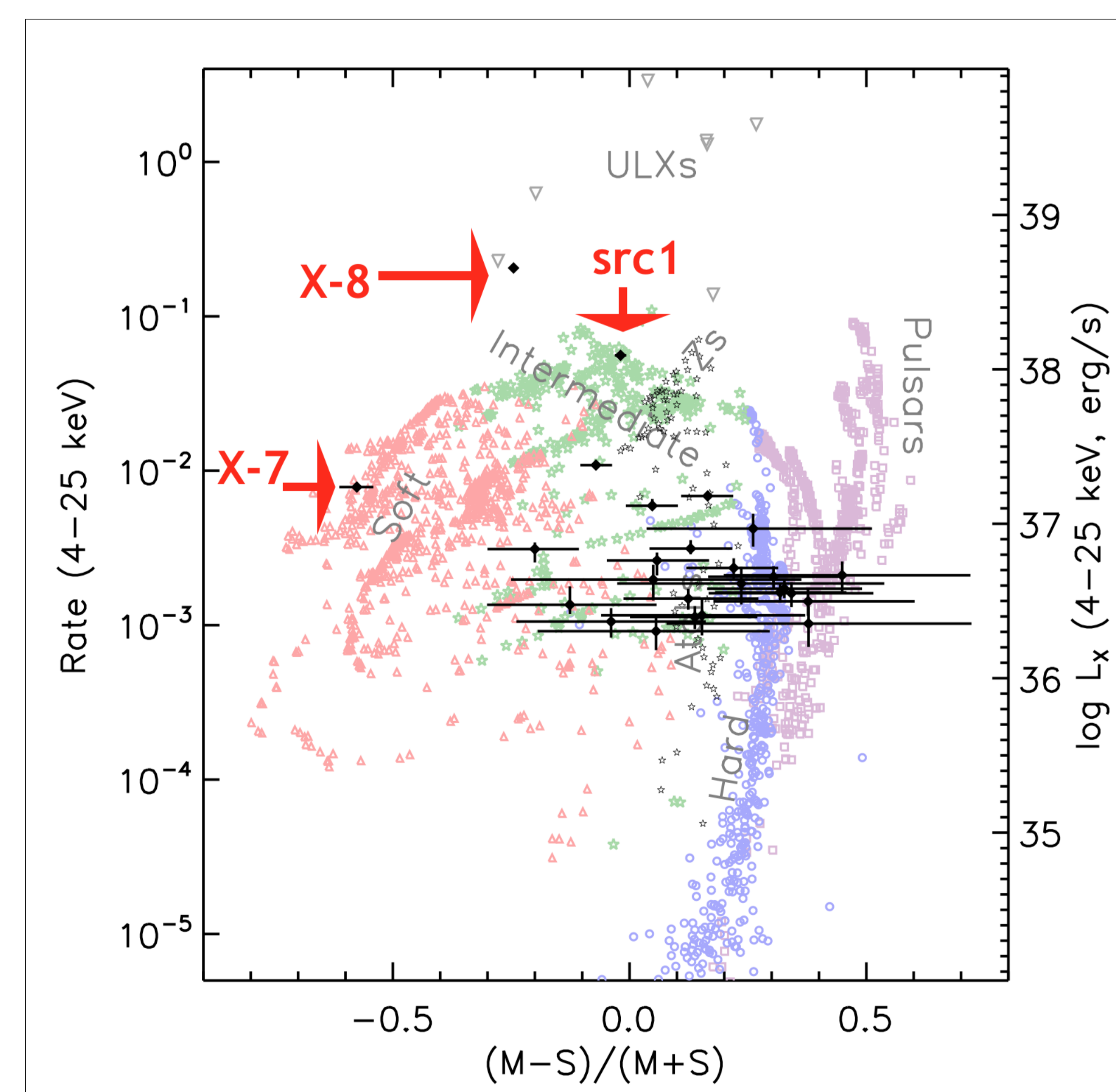


Figure 3: **Hardness-intensity diagram** for X-ray sources in **M33** (black square), and pulsars, hard/intermediate/soft-state BH XRBs in the Milky Way (magenta, blue, green, red symbols) and Ultraluminous X-ray sources (ULXs) studied by NuSTAR (gray upside-down triangles). The hardness ratio is from $M = 6-12$ keV and $S = 4-6$ keV band count-rates. My surveys thus far constrain the accretion-state distributions for luminous XRB populations in M33. These M33 observations constrain the distribution of accretion states for a low-luminosity HMXB-rich population.

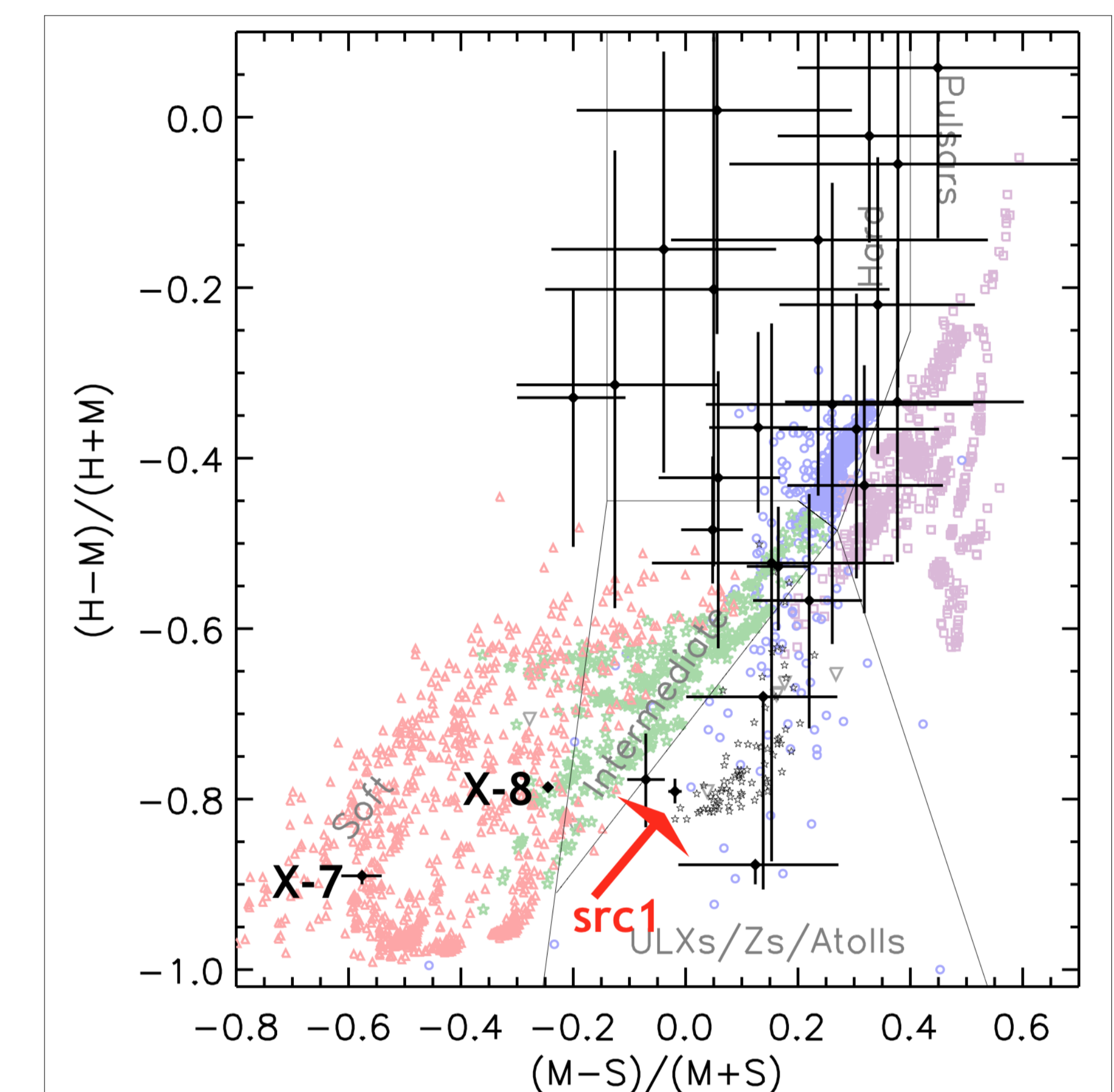


Figure 4: **Color-color diagram**. The black squares with error bars are the 28 sources in M33.

M33 X-8

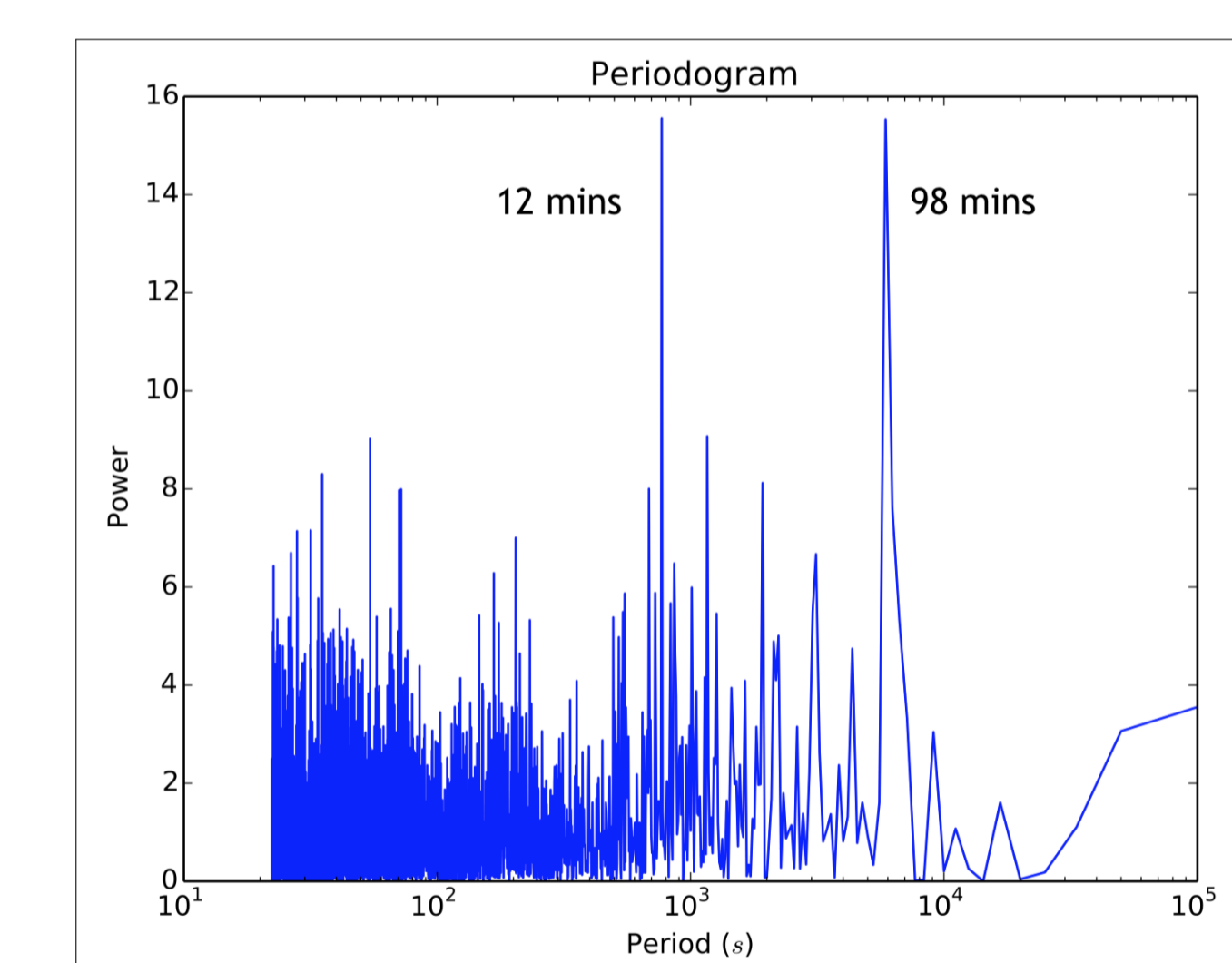


Figure 5: NuSTAR: 50310002001. Pulsations: Instrument A 99.46 ± 5.6 mins, 12.82 ± 0.1 mins; Instrument B 100.2 ± 5.68 mins, 12.08 ± 0.09 mins.

Conclusion

In contrast to a similar NuSTAR survey of M31 (with a low-mass XRB-dominant population), the source population is dominated by high-mass XRBs, allowing the study of a very different population with similar sensitivity. These results provide a significant improvement in our knowledge of **high-mass XRB accretion states** that proves valuable for theoretical XRB population synthesis studies.

Contact Information

Email: yangjun@mit.edu Web: <http://www.jyang.us>